

Cuprate core level line shapes for different Cu-O networks

K. Karlsson^{1,2}, O. Gunnarsson² and O. Jepsen²

⁽¹⁾*Inst. för Naturvetenskap, Höskolan Skövde, S-541 28 Skövde, Sweden*

⁽²⁾*Max-Planck-Institut für Festkörperforschung, D-70506 Stuttgart, Germany*
(July 18, 2018)

We have studied the Cu core level photoemission spectra in the Anderson impurity model for cuprates with different Cu-O networks, dimensionalities (zero, one, two and three) and Cu valencies (two and three). We focus on the shape of the leading peak and obtain very good agreement with the experimental data. We show how the shape of the spectrum is related to the valence electronic structure and the Cu-O network but also that other atoms can play a role.

Böske *et al.* [1] have shown that for a number of Cu compounds the shape of the *core* level photoemission spectrum strongly depends on the type of Cu-O network. This illustrates that it is not sufficient to think of the core level spectra as primarily atomic-like, but that there is a substantial influence from the valence electron structure. The core level spectrum can therefore give interesting information about the electronic structure.

The Cu compounds studied by Böske *et al.* are divalent, with Cu having mainly d^9 character. When a Cu core hole is created, it is energetically favorable to transfer an electron from the surrounding to the site of the core hole, forming a d^{10} state. This leads to a spectrum with a leading peak of primarily d^{10} character and a satellite of mainly d^9 character [2]. The main peak corresponds to a process where an electron has hopped from the valence band to the site with a core hole, and its shape reflects the valence band structure [3,4]. This leads to a broadening of the main peak and possibly to further structures. Early experiments with a moderate resolution showed little structure. The high-resolution experiments of Böske *et al.* [1], however, reveal a clear system dependence of the core level spectra. In the present paper we calculate these spectra and show that they are in good agreement with experiment. We explain in detail the origin of the differences between different cuprates. It has been suggested that the shape of the leading peak is explained in terms of a two-peak structure, due to so-called local and nonlocal screening [5]. The recent experiments, however, show that the shape can be substantially more complicated.

To calculate the core spectrum, we use the Anderson impurity model

$$H = \sum_{\nu=1}^{10} \left\{ \int \varepsilon \psi_{\varepsilon\nu}^\dagger \psi_{\varepsilon\nu} d\varepsilon + [\varepsilon_d - U_{dc}(1 - n_c)] \psi_\nu^\dagger \psi_\nu \right. \\ \left. + \int [V_\nu(\varepsilon) \psi_\nu^\dagger \psi_{\varepsilon\nu} + h.c.] d\varepsilon \right\} + U \sum_{\nu < \mu} n_\nu n_\mu, \quad (1)$$

where ν is a combined spin and orbital index. The (host) valence states are labelled by the energy ε and ν , and the Cu impurity $3d$ states are labelled by ν [6]. The impurity level is pulled down from ε_d to $\varepsilon_d - U_{dc}$ when a core

hole is created. The electrons on the impurity have the Coulomb repulsion U .

It is crucial to use realistic hopping matrix elements $V_\nu(\varepsilon)$. The local density of states (LDOS) $\rho_\nu(\varepsilon)$ of a $3d$ orbital with the label ν is calculated for all compounds studied here, using the the local density approximation (LDA) and the LMTO method [7]. Then [8]

$$\pi |V_\nu(\varepsilon)|^2 = -\text{Im} \left\{ \left[\int d\varepsilon' \frac{\rho_\nu(\varepsilon')}{\varepsilon - \varepsilon' - i0} \right]^{-1} \right\}. \quad (2)$$

An Anderson impurity calculation using these matrix elements contains effects of all the $3d$ orbitals, not just the ones on the impurity. An *impurity* calculation with $U = 0$ exactly reproduces the LDOS of a *lattice* band structure calculation [8]. In our calculation with $U \neq 0$, the many-body effects are treated explicitly on the site where the core hole is created, while it is assumed that the $3d$ states on the other sites can be treated in the LDA. In the discussion of the Anderson impurity model, it is often overlooked that all $3d$ states are (approximately) included.

We set $U = 8$ eV and $U_{dc} = 10$ eV [4], and adjust ε_d so that the relative weights of the main peak and the satellite agree with experiment. We have neglected multiplet effects. These effects are important for the shape of the satellite, but not for the shape of the main peak, which we consider here.

To solve the model, we expand the ground-state as [10]

$$|E_0\rangle = A(\psi_\nu |d^{10}\rangle + \int^{\varepsilon_F} d\varepsilon a(\varepsilon) \psi_{\varepsilon\nu} |d^{10}\rangle), \quad (3)$$

where the parameters A and $a(\varepsilon)$ are determined variationally. $|d^{10}\rangle$ is a state with all the valence states ($|\varepsilon\nu\rangle$) up to the Fermi energy (ε_F) as well as all the impurity states filled. The first term in (3) corresponds to a d^9 configuration and the second to a state where a valence electron with the energy ε has filled the $3d$ -hole, in the following referred to as $d^{10}\varepsilon^{-1}$. Then

$$a_\nu(\varepsilon) = \frac{V_\nu(\varepsilon)}{\Delta E - \varepsilon_d + \varepsilon}. \quad (4)$$

ΔE is the lowering of the total energy due to hopping relative to the energy of the d^9 state. Typically $|\Delta E - \varepsilon_d|$

is of the order of a few eV. A lowering of ε leads to a decrease of $a(\varepsilon)^2$, unless the variation of the denominator is compensated by a strong energy dependence of $|V(\varepsilon)|^2$. By adding more states to the Ansatz (3), the model can be solved increasingly accurately. However, the effect of additional states is essentially just a renormalization of ε_d , which we treat as an adjustable parameter anyhow. The core level spectrum is calculated, by using a resolvent operator and by inserting intermediate states similar to the two terms in Eq. (3) [10,6]. The spectra were broadened by a Lorentzian (FWHM=1.1 eV) to simulate life-time effects and by a Gaussian (FWHM=0.4 eV) to simulate the instrumental broadening.

The results are shown in Fig. 1, and they are in very good agreement with the experiments of Böske *et al.* [1]. In agreement with experiment, $\text{Ba}_3\text{Cu}_2\text{O}_4\text{Cl}_2$ and Li_2CuO_2 have very narrow peaks, Bi_2CuO_4 a slightly broader peak and the remaining compounds significantly broader spectra. The shoulder of SrCuO_2 is more pronounced than for Sr_2CuO_3 , as it should, and the three peak structure of $\text{Ba}_2\text{Cu}_3\text{O}_4\text{Cl}_2$ is reproduced very well. The main difference to experiment is that the leading structure of $\text{Sr}_2\text{CuO}_2\text{Cl}_2$ is narrower. The high binding energy structures of Sr_2CuO_3 and SrCuO_2 furthermore occur at somewhat lower binding energy and the high binding energy structure of SrCuO_2 is somewhat more pronounced.

We now discuss the shape of the spectra. In the presence of a core hole, the $d^{10}\varepsilon^{-1}$ configuration is significantly lower in energy than the d^9 configuration. For the qualitative discussion (but not in the calculations) we assume that the coupling between these configurations can be neglected in the final state. Although this underestimates the weight of the leading peak, it reproduces its shape quite well (compare ‘Spectrum’ and ‘ $a^2(\varepsilon)$ ’ in Fig. 2). The corresponding spectrum is

$$\rho(\varepsilon) = A^2[a^2(\varepsilon)\Theta(-\varepsilon) + \delta(\varepsilon - \varepsilon_d + U_{dc})], \quad (5)$$

where the first term gives the main peak and the second the satellite. The shape of the main peak is then determined by $a^2(\varepsilon)$, which is related to $|V(\varepsilon)|^2$ via Eq. (4). We therefore first study the relation between $V(\varepsilon)$ and the electronic structure.

$V(\varepsilon)$ gives the hopping between the impurity and host (the rest of the solid but with the impurity removed). We first consider the case when the LDOS $\rho_\nu(\varepsilon)$ in Eq. (2) is given by a semi-ellipse

$$\rho_\nu(\varepsilon) = \frac{2}{\pi B^2} \sqrt{B^2 - \varepsilon^2} \quad |\varepsilon| \leq B, \quad (6)$$

where $2B$ is the width of the band. Performing the Hilbert transform in Eq. (2) then gives the same shape

$$\pi|V_\nu(\varepsilon)|^2 = \frac{1}{2\pi} \sqrt{B^2 - \varepsilon^2} = \frac{B^2}{4} \rho_\nu(\varepsilon) \quad |\varepsilon| \leq B. \quad (7)$$

The overall strength of the hopping is determined by the width of the LDOS. This is expected, since a large width of the LDOS implies a strong hopping.

The most important energy bands in the cuprates studied here consist of antibonding combinations of one Cu orbital (e.g., $x^2 - y^2$) with p orbitals on the neighboring O sites located around ε_F and corresponding bonding combinations some 5-6 eV below ε_F . The bonding-antibonding splitting is mainly determined by the Cu-O hopping, while the width of the two bands mainly depends on the hopping to more distant CuO_n units. As a model for the LDOS we use two semi-ellipses

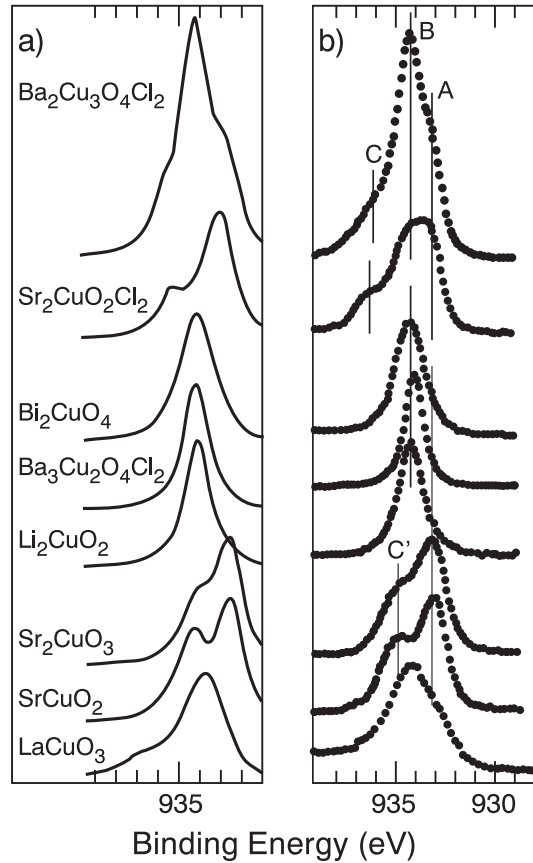


FIG. 1. a) Theoretical core level spectra for different divalent and one trivalent (LaCuO_3) cuprate. The figure only shows the main peak, while the satellite at higher binding energies is not shown. b) Experimental spectra by Böske *et al.* [1] for the divalent Cu compounds and by Mizokawa *et al.* [11] for the trivalent LaCuO_3 .

$$\rho_\nu(\varepsilon) = \alpha \frac{2}{\pi B^2} \sqrt{B^2 - \varepsilon^2} \Theta(B^2 - \varepsilon^2) + (1 - \alpha) \frac{2}{\pi B^2} \sqrt{B^2 - (\varepsilon - \varepsilon_0)^2} \Theta(B^2 - (\varepsilon - \varepsilon_0)^2). \quad (8)$$

This LDOS may result in a δ -function between the two continuous parts of the LDOS. If $\alpha|\varepsilon_0| \gg B$ and $(1 - \alpha)|\varepsilon_0| \gg B$, there is a δ -function at $\varepsilon = \alpha\varepsilon_0$ with the weight $\pi\alpha(1 - \alpha)\varepsilon_0^2$. This corresponds to the coupling to a linear combination of p orbitals on the neighboring O

atoms. The position of the δ -function depends, however, on the weights and widths of the bonding- and antibonding bands. In addition, there is a continuous part at the bonding and antibonding bands with a strength that is related to the widths of these bands. In practice, the LDOS is not zero between the bonding- and antibonding bands, and the δ -function then has a broadening.

In Fig. 2 we show results for $\text{Ba}_2\text{Cu}_3\text{O}_4\text{Cl}_2$, which has two inequivalent Cu atoms (Cu_A and Cu_B). One of the Cu atoms (Cu_B) is connected to neighboring Cu_B atoms only via Cu-O-O-Cu bond and to neighboring Cu_A atoms via 90° Cu-O-Cu bond angles. Neighboring Cu atoms then couple to different O p orbitals, and they only have a weak coupling via other orbitals. The bonding- and antibonding bands are therefore narrow, as illustrated by the panel LDOS in Fig. 2a. The resulting $|V(\epsilon)|^2$ has a broadened δ -function between the bands but very little weight at the energies of the bands. The corresponding $a^2(\epsilon)$ also has most of the weight between the two bands. This shape agrees well with the result of the full calculation (without the approximation (5)), and explains the narrow peak in the core level spectrum from Cu_B . The other Cu atom (Cu_A) is connected to the neighboring Cu atoms via 180° Cu-O-Cu bond angles. Neighboring Cu atoms then couple to the same O p orbital, i.e., they have a strong coupling. As a result, in particular the antibonding band is broad, as illustrated by the LDOS in Fig. 2b. The corresponding $|V(\epsilon)|^2$ has a broadened δ -function, which is shifted towards lower energies than for Cu_B , due to the different widths and weights of the two bands. In particular, however, there is a substantial coupling in the energy range of the antibonding band. This coupling is strongly enhanced by the energy denominator ($\Delta E - \epsilon_d + \epsilon$) of Eq. (4) in the calculation of $a(\epsilon)$. Therefore, this coefficient is rather large for small binding energies. Due to a structure in $|V(\epsilon)|^2$ at $\epsilon \sim -2$ eV, $a^2(\epsilon)$ also has a structure at this energy. Finally, the large structure in $|V(\epsilon)|^2$ at $\epsilon \sim -4$ eV leads to a third structure in the spectrum. Adding the spectra from Cu_A and Cu_B gives the spectrum in Fig. 1.

Following the analysis in Fig. 2, we divide the systems in roughly two classes. One class consist of systems where the CuO_4 units have a weak coupling to the other CuO_4 units, either due to the Cu-O-Cu bond angles being (rather close to) 90° or because the systems is approximately zero-dimensional (0d). In the second class the CuO_4 units have a strong coupling to other CuO_4 units, due to Cu-O-Cu bond angles of the order of 180° .

Bi_2CuO_4 (0d), $\text{Ba}_3\text{Cu}_2\text{O}_4\text{Cl}_2$ and Li_2CuO_2 belong to the first class. We would then expect a narrow peak in the core spectrum, occurring at a higher binding energy than the leading edge. This is confirmed for the latter two systems, while both theory and experiment shows a somewhat broader peak for Bi_2CuO_4 . The reason for this is that there is a coupling between the CuO_4 units via the Bi atoms. As a result the structure in $|V(\epsilon)|^2$

between the bonding- and antibonding bands is broader, leading to a somewhat broader core level spectrum. This illustrates that not only the Cu-O network plays a role.

$\text{Sr}_2\text{CuO}_2\text{Cl}_2$, Sr_2CuO_3 and SrCuO_2 belong to the second class. In the two-dimensional (2d) structures $\text{Ba}_2\text{Cu}_3\text{O}_4\text{Cl}_2$ (Cu_A) and $\text{Sr}_2\text{CuO}_2\text{Cl}_2$ the antibonding band is broader than in the 1d structures Sr_2CuO_3 and SrCuO_2 , due to the more efficient hopping to neighboring CuO_4 units in the 2d case. Therefore, the structure in $|V(\epsilon)|^2$ at $\epsilon \sim -2$ eV is broader and the peak in $|V(\epsilon)|^2$ at $\epsilon \sim -4$ eV has been pushed to somewhat lower energies in the 2d case. The large binding energy structure in the main peak is then pushed towards somewhat larger energies in the 2d case, in agreement with experiment (see C and C' in Fig. 1).

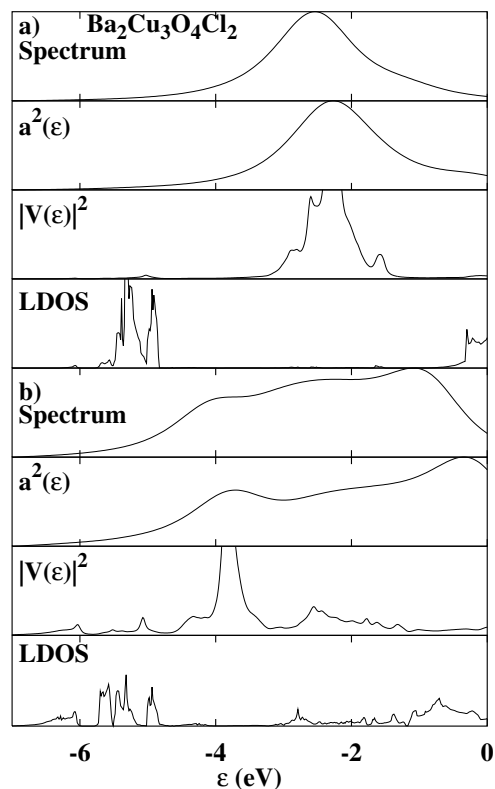


FIG. 2. Core level spectrum, broadened $a^2(\epsilon)$, $|V(\epsilon)|^2$ and local density of states (LDOS) for the two (a) and b)) inequivalent Cu atoms in $\text{Ba}_2\text{Cu}_3\text{O}_4\text{Cl}_2$. $|V(\epsilon)|^2$ and the LDOS have been given a small (FWHM=0.03 eV) broadening, while $a^2(\epsilon)$ has been given the same broadening as the spectrum. We have put $\epsilon_F = 0$.

Above we have considered divalent Cu. We have earlier studied the trivalent NaCuO_2 , and found that this has a narrow leading peak due to a narrow structure in $|V(\epsilon)|^2$ [4]. An alternative explanation was suggested by a cluster calculation, where it was argued that the reason for the small width is the valence (3+) [5]. We have therefore considered a different trivalent compound, namely

LaCuO₃. The corresponding spectrum is shown at the bottom of Fig. 1. The main peak is broad, both according to theory and experiment [11]. The reason is similar as for the broad peaks in the divalent compounds, namely a broad antibonding band due to a Cu-O-Cu bonding angle of about 180°. Due to the three-dimensional character of this compound, the band is unusually broad, but only a relatively small fraction is occupied, because the compound is trivalent. Therefore the broadening of the leading peak is only modest. If we had instead studied a model of the type used in the cluster calculations, with only one orbital per atom, the antibonding band would have been empty. The Anderson impurity model would then have predicted a narrow leading peak, as the cluster calculations do. To obtain the correct description of LaCuO₃ it is therefore crucial to use a realistic model which includes the partial filling of the antibonding band, and which goes beyond the normally used cluster models.

In an exact diagonalization treatment of a Cu₃O₁₀ cluster, the leading peak consists of two δ -functions. These correspond to so-called local and nonlocal screening [5], indicating that the charge screening of the core hole comes from the closest O₄ unit or from the neighboring CuO₄ units, respectively. Similar results are obtained in the Anderson impurity model for such a cluster. Finding the solutions of the host, we notice that the highest occupied level has a strong antibonding character and is located on the neighboring CuO₄ units. The second highest occupied level (with a coupling to the impurity) has a large weight on the O₄ unit around the impurity. Due to the missing hybridization with the impurity, this host level is less antibonding and lower in energy. The two δ -functions in the spectrum essentially correspond to an electron from one of these two host levels hopping into the impurity orbital. Due to their different characters, these levels give local or nonlocal screening.

It has been emphasized that it is important to take into account the formation of a Zhang-Rice singlet on the CuO₄ units neighboring the unit with a core hole [5]. We find that in the Anderson impurity model of a Cu₃O₁₀ cluster, the two lowest final states contain comparable amounts of a Zhang-Rice singlet as is found in exact diagonalization for such a cluster. If the highest occupied host level is emptied, a large amount of antibonding character is removed from the neighboring CuO₄ units. This alone is enough to give a large overlap to a state with a Zhang-Rice singlet on one of these units. If instead the second highest host level is emptied, the screening charge is primarily taken from the local O₄ unit, and the local singlet character on the neighboring CuO₄ units remains small.

To further test the role of the singlet in core level photoemission, we have performed a calculation for a Cu₃O₁₀ cluster with 25 valence electrons. This system has only one valence hole, and a Zhang-Rice singlet cannot form. The change of the number of electrons gives a somewhat

different spectrum, but the main peak still has a substantial broadening, illustrating that just going beyond a single site model (CuO₄) leads to a broadening of the leading peak. The considerations above illustrate the usefulness of a picture where an electron from a host level hops into the impurity orbital.

It has been found that even rather ‘large’ clusters like Cu₃O₁₀ may not be converged with respect to their size [12]. The inclusion of additional orbitals like O p_π may also be important [12]. Here we have found further examples of a need for more realistic models, e.g., for Bi₂CuO₄ and LaCuO₃. In an exact diagonalization approach, however, it is not possible to make the cluster much larger or to add many other orbitals, since the many-electron space then becomes too large, while such a system can be treated in the Anderson impurity approach.

To summarize, we have calculated core level spectra for a number of cuprates in the Anderson impurity model using *ab initio* hopping matrix elements. In this way, many-body effects are treated explicitly for the Cu site where the core hole is created, while the other Cu sites are treated in the LDA. This model gives a very good agreement with experimental core level spectra. The shape of the leading peak is influenced substantially by the valence electronic structure and thereby the lattice structure. The presence of (approximately) 180° Cu-O-Cu bond angles leads to a broad and structured leading peak, and an increase in the dimension of the Cu-O network tends to increase the width. In particular for the trivalent compounds, it is important to go beyond the simple cluster models with one orbital per site, since these models always give a narrow leading peak.

This work has been supported by the Max-Planck-Forschungspreis.

-
- [1] T. Böske, K. Maiti, O. Knauff, K. Ruck, M.S. Golden, G. Krabbes, J. Fink, T. Osafune, N. Motoyama, H. Eisaki, and S. Uchida, Phys. Rev. B **57**, 138 (1998).
 - [2] A. Kotani and Y. Toyozawa, J. Phys. Soc. Japan, **37**, 912 (1974); **35**, 1073 (1973); **35**, 1082 (1973).
 - [3] O. Gunnarsson and K. Schönhammer, Phys. Rev. Lett. **41**, 1608 (1978).
 - [4] K. Karlsson, O. Gunnarsson, and O. Jepsen, J. Phys.: Condens. Matter **4**, 895 (1992).
 - [5] M.A. van Veenendaal and G.A. Sawatzky, Phys. Rev. Lett. **70**, 2459 (1993); Phys. Rev. B **49**, 3473 (1994); M.A. van Veenendaal, H. Eskes, and G.A. Sawatzky, Phys. Rev. B **47**, 11462 (1993).
 - [6] O. Gunnarsson and K. Schönhammer, in *Handbook of the Physics and Chemistry of the Rare Earths* Vol. 10, Eds. K.A. Gschneider, Jr., L.R. Eyring, and S. Hüfner, North-Holland, Amsterdam, 1987, p. 103.

- [7] O.K. Anderson, Phys. Rev. B **12**, 3060 (1975); O.K. Anderson and O. Jepsen, Phys. Rev. Lett. **53**, 2571 (1984).
- [8] O. Gunnarsson, O.K. Andersen, O. Jepsen, and J. Zaanen, Phys. Rev. B **39**, 1708 (1989).
- [9] O. Gunnarsson, O. Jepsen, and Z.-X. Shen, Phys. Rev. B **42**, 8707 (1990).
- [10] O. Gunnarsson and K. Schönhammer, Phys. Rev. Lett. **50**, 604 (1983); Phys. Rev. B **28**, 4315 (1983).
- [11] T. Mizokawa, T. Konishi, A. Fujimori, Z. Hiroi, M. Takano, and Y. Takeda, J. Elec. Spec. Rel. Phen. **92**, 97 (1998); T. Mizokawa, A. Fujimori, H. Namatame, Y. Takeda, and M. Takano, Phys. Rev. B **57**, 9550 (1998).
- [12] K. Okada and A. Kotani, Phys. Rev. B **52**, 4794 (1995).